A Study on the Relationship between the Signal Characteristic of Electromagnetic Acoustic Transducer (EMAT) and the Defect style of cylindrical pipe

M. K. Chang*, L. L. Shen, Z. L. Lin, F. C. Chi
Department of Safety Health and Environment Engineering, National Yunlin University of Science and Technology (NYUST), Yunlin 64002, Taiwan, R.O.C.

Abstract
Electromagnetic acoustic transducer (EMAT) is non-contact, without coupling operation, and suitable for testing at high temperature or defects at rough pipeline surface. This study aimed to detect the artificial pipeline by using EMAT, and to explore the relation between the defect and signal. By measuring the signal amplitude, we discovered that the length of the defect increases with the amplitude attenuation and the depth of defect will affect the amplitude attenuation. In addition, the amplitude attenuation will increase with flat-bottomed hole area of the defect obviously. This study showed that the signal amplitude attenuation of EMAT can be affected by the defect depth, the defect length, and the hole area of the pipeline. According to the experimental results, this study can significantly improve the detection accuracy of pipeline defects, and will serve as a reference for engineers assessed.

Keywords: Non-destructive testing (NDT), Ultrasonic testing, Manual defect, Electromagnetic acoustic transducer (EMAT)

1. INTRODUCTION
The conventional ultrasonic testing produces wave detection, which is affected by energy attenuation, in media transfer process[1]. Therefore, its long-distance detecting is limited. Because the electromagnetic acoustic transducer (EMAT) generates the Lamb waves which have the peculiarity of rapid transfer and wave propagation distance, the wave energy will not decay for meters[2], and is highly sensitive towards the variation of the object thickness. Without mobile equipment and the removal of pipeline coating, such as fixed-point, the measuring can be remote completed by sending out the Lamb wave towards object at far distance. Cracks detection experiments were completed by this system, and the detection error of cracks location was less than 1 %. The whole system could run reliably, and could be used for steel cracks detection[11].

In this study, we fabricated different defected samples of pipelines to simulate the defected piping in construction site. Then the flawed pipeline was detected by EMAT and the relationship between defect and signal was probed:

a. Effects of different depth and length of flaws on a signal amplitude.
b. Effects of various circumferential flaws on a signal amplitude.
c. Effects of different flat-bottomed hole flaws on a signal amplitude.

2. EXPERIMENTAL PRINCIPLE

EMAT generates the Lamb wave and shares horizontal wave (SH-wave) transducer by magnetostrictive force, as shown in Figure 1. The magnetic field of the magnet and the coil produces an alternating magnetic field, and then high-frequency current pulse is used into the coil through high-frequency alternating magnetic field, and an electromagnet that creates a static bias magnetic field superimpose and generates alternating magnetic field. The magnetic material volume are changed and the formation of inside vibration. Finally the forming waves are spread[3]. Figure 1 (a) shows that the direction of the particle vibration is perpendicular to that of the sound wave propagation, parallel to the material surface, and thus less affected by the surface. Figure 1 (b) shows that particle vibration is parallel to the direction of sound wave propagation. Therefore, the affection by the surface and decay is obvious.[1-5]

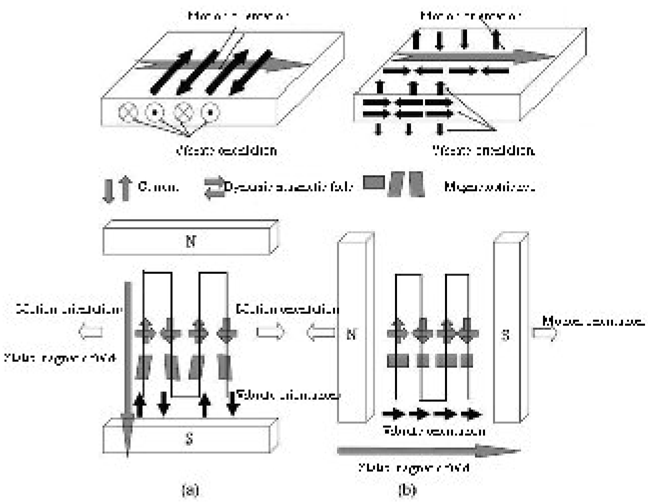

Figure 1: Use of magnetostrictive force actuators for EMAT(a) SH-wave; (b) Lamb wave【Riichi, 2004】.

3. EXPERIMENTAL METHODS

3.1. Materials

The experiment used four 4-inch carbon steel pipes (ASTM A106) with diameter of 11.4 cm, wall thickness of 0.65 cm, and circumference of 36.0 cm. To produce defects milled with the depth of 1/2 T, where T is the wall thickness, and defect length is 4 cm, as shown in Figure 2. The defects with the depth of 1/2 T and 1/4 T, and defect length was 15cm as shown in Figure 3. Figure 4 shows the angle for circumferential defects are, 90°, 180°, 270°, and 360°. The defect is depth is 1/2 T, and flat-bottomed hole diameters are 4φ, 2*2φ, 2φ, and 1φ (cm), as shown in Figure 5.

Besides, used nine 6-inch carbon steel pipes (ASTM A106) with diameter of 16.75 cm, wall thickness of 0.75 cm, and circumference of 53.0 cm. To produce defects milled with the depth of 1/2 T and 1/4 T, and defect length is 4 cm, as shown in Figure 6 and 7. The defects with the depth of 1/2 T and 1/4 T, and defect length was 15cm, as shown in Figure 8 and 9. Figure 10 shows the angle for circumferential defects are 45°, 90°, 120°, 135°, 180°, 270°, and 360°. The defect is depth is 1/2 T, and flat-bottomed hole diameters are 4φ, 2*2φ, 2φ, and 1φ (cm), as shown in Figure 11.

3.2 Detection method

In this study we used EMAT Scans software to display the signals under Do Runs mode. The Do Runs mode records graphics by scanning the phase and amplitude. Figure 12 demonstrates the Lamb wave propagation in T1 path from exciter coils to receiver coils. The changes of T1 amplitude signal in the defects were determined by computer. The Do RUNS measured the amplitude signal as delineated in Figure 13.

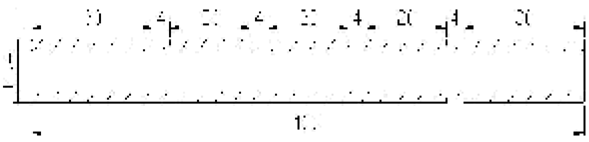

Figure 2: Defect length of 4 cm in the 4-inch pipe.

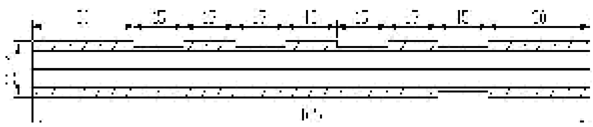

Figure 3: Defect length of 15 cm in the 4 inch pipe.

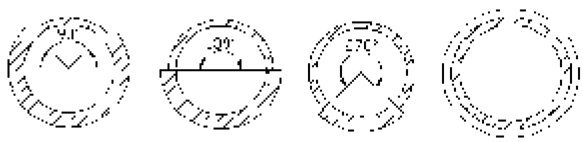

Figure 4: Artificial circumferential defects made on pipe surfaces.

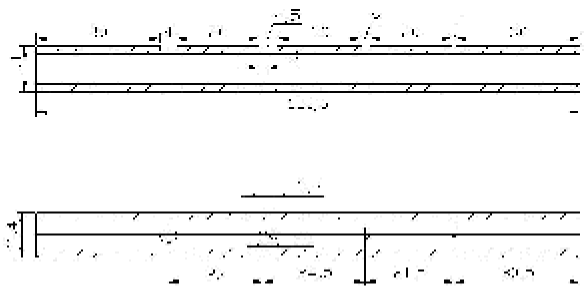

Figure 5: Flat-bottomed holes in the 4 inch pipe.

Figure 6: Defect length of 4 cm in the 6-inch pipe.

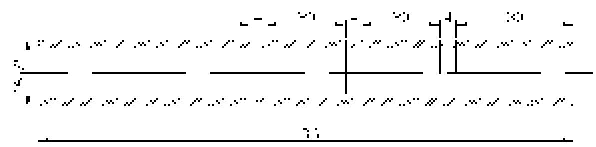

Figure 7: Defect length of 4 cm in the 6-inch pipe.

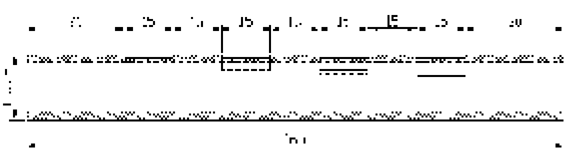

Figure 8: Defect length of 15 cm in the 6-inch pipe.

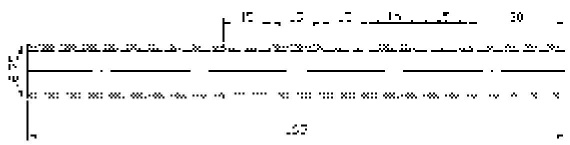

Figure 9: Defect length of 15 cm in the 6-inch pipe.

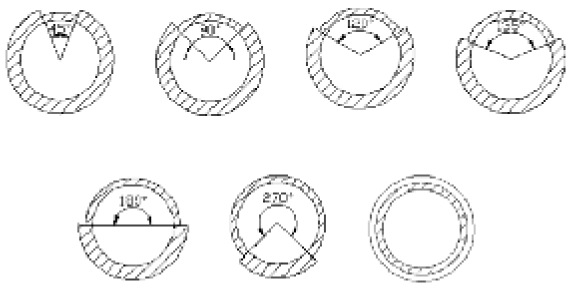

Figure 10: Artificial circumferential defects made on pipe surfaces..

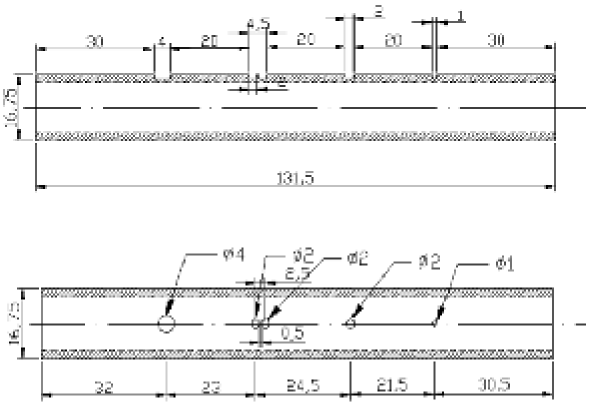

Figure 11: Flat-bottomed holes in the 6 inch pipe.

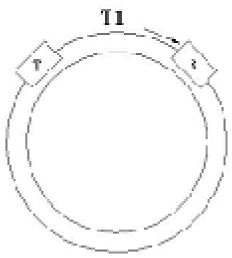

Figure 12: The Lamb wave propagation path.

signal

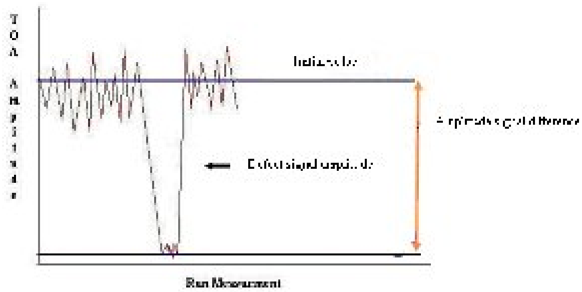

Figure 13: The Do RUNS measured the amplitude

4. RESULTS AND DISCUSSION

4.1. The Same Depth Defects, Defects of Different Length in the 4-inch pipe

4.1.1. T1 Result for Different Lengths (1/2 T; 4 L & 15 L) in the Same Depth

In the Figure 14 at circumferential angle 90 and 180° defects, the measured signal displays a positive linear relationship. The signal was degraded by interference from the wave propagation ran into the 270 and 360° defects, and the difference of the signal amplitude was less than circumferential angle 180° defect. For the same defect depth of 1/2T, the defect length of 15 cm amplitude signal difference was more predominantly than 4 cm.

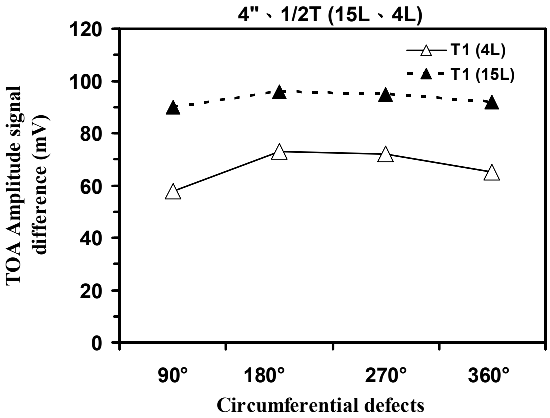

Figure 14: 1/4 T (depth), 4 cm &15 cm (length), Top (direction), T1 (path) of 4-inch pipe

4.2. The Same Length Defects, Defects of Different Depth in the 4-inch pipe

4.2.1. T1 Result for Different Depth (15L; 1/2T & 1/4T) in the Same Length

The measured defects for the circumferential angles were 90°, the sound wave will first contact with the wall without defects, then touch the defect occur changes in acoustic impedance, and contact with the wall without defects again before return to receiver transducer. So the difference of the signal amplitude was less than 180° defects. For the same defect length of 15 cm, the 1/2T depth amplitude signal difference was more predominantly than the 1/4 T depth, as shown in Figure 15.

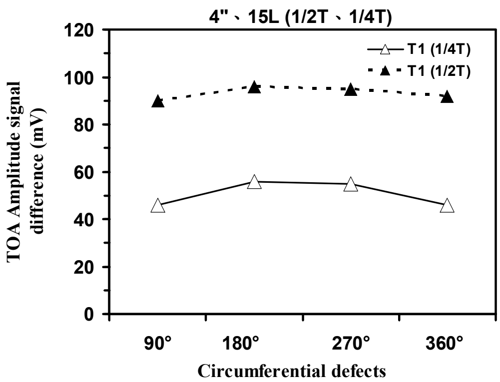

Figure 15: 1/4 T & 1/2 T (depth), 15 cm (length), Top (direction), T1 (path) of 4-inch pipe

4.3. The Same Depth Defects, Defects of Different Length in the 6-inch pipe

4.3.1 T1 Result for Different Lengths (1/2 T; 4 L & 15 L) in the Same Depth

The circumferential angle of two transducers was about 102°. As a result, when the measured defects for the circumferential angles were 45 and 90°, the sound wave will first contact with the wall without defects, then touch the defect occur changes in acoustic impedance, and contact with the wall without defects again before return to receiver transducer. For the 45 and 90° defects, the defect signal amplitude was higher than others. In the Figure 16 at 45 and 90° defects, the measured signal displays a positive linear relationship. The amplitude signals show a approximate constant value, when circumferential defect distance between the two transducers was greater than 102°. For the same defect of 1/2 T depth, the difference of the long defect amplitude signals is more predominantly than the short one by T1.

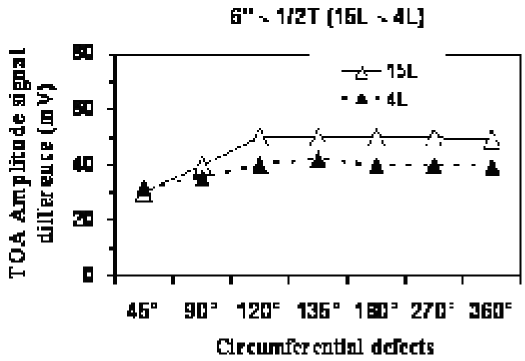

Figure 16: 1/2 T (depth), 4 cm & 15 cm (length), Top (direction), T1 (path) of 6-inch pipe

4.4. The Same Length Defects, Defects of Different Depth in the 6-inch pipe

4.4.1 T1 Result for Different Depth (4L; 1/2T & 1/4T) in the Same Length

The circumferential angle 45°-135° defect and amplitude signal differences were in a proportional relationship. The 135°–360° circumferential defects and amplitude signal difference were about a fixed value. This is due to the circumferential defect of the angle and the two transducer distances. For the same defect length of 4 cm, the 1/2T depth amplitude signal difference was more predominantly than the 1/4 T depth, as shown in Figure 17. Therefore, the deeper of the depth, the greater difference of amplitude signals by T1.

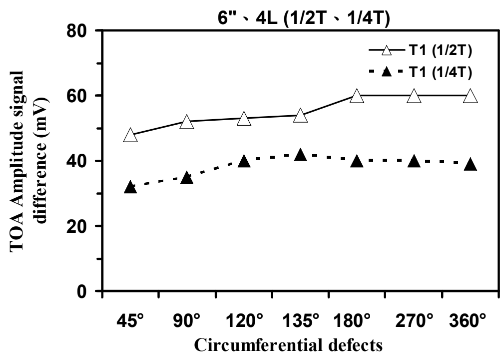

Figure 17: 1/4 T & 1/2 T (depth), 4 cm (length), Top (direction), T1 (path) of 6-inch pipe

4.5. Effects of the Signal Amplitude on Different Flat-bottomed Hole Defects.

As the hole diameter increased, the defect signal amplitude was significant. The signal was degraded by interference from the wave propagation ran into the two short range defects (2*2φ), as shows in Figure 17. The difference of the signal amplitude was more than 2 cm and less than 4 cm for 6 inch. But for 4 inch, the difference of the signal amplitude was more than 2 cm and 4 cm. For T1 signal map, the difference of amplitude signals increased with the hole area.

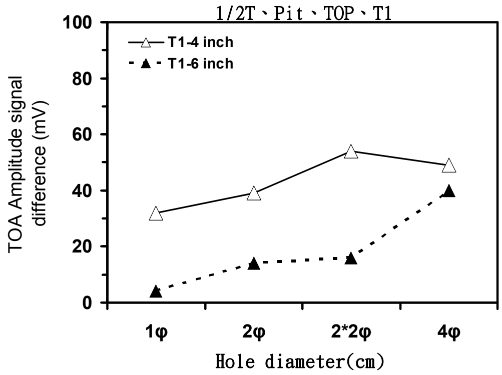

Figure 18: The flat-bottomed hole defect depth of 1/2 T, Top (direction), T1 (path).

5. CONCLUSION

To understand the comparison and analysis of various pipeline flaw signals by EMAT, in this study, we used 4-inch and 6-inch cylinder to make different defect lengths, defect depths and sizes of the flat-bottomed holes. Then we detected the defect pipelines by EMAT and investigated the signals of the different defects within pipe. With the increase of the defect length, the defect signal amplitude was predominant by EMAT for the same defect depth. However, the defect depth also affected the amplitude attenuation when the defect length was fixed. Measuring the pipeline corrosion defects is feasible by EMAT. As the pipeline hole area increased, the defect signal amplitude was significant. The EMAT for the detection of pitting corrosion in site was in good capability of inspection.

In this study we inspected the pipeline no content objects. Suggestions for future research could explore the different fluid types and flow of pipeline, testing of the EMAT signal amplitude attenuation characteristics. In the future to overcome the difficulties of making the defect, and inspect the pipeline by EMAT. It will contribute to the operator to quickly identify the characteristics of the defect of inside and outside in the field.

References

1. J. J. Shia, Electromagnetic ultrasonic testing Introduction, NDT, 26, 6, (2004).
2. Y. H. Cheng, Pipeline inspection using lamb waves, National Sun Yat-sen University, (2001).
3. R. Murayama, S. Makiyama, M. Kodama, and Y. Taniguchi, Development of an ultrasonic inspection robot using an electromagnetic acoustic transducer for a Lamb wave and an SH-plate wave, Ultrasonic, 42,825-859 (2004).
4. S. H. Lin, The study of applying Electro Magnetic Acoustic Transducer (EMAT) to detect flaw within cylinder pipe, NYUST (2009).

5. Y. J. Chen, and H. Y. Deng, Non-destructive testing, Chaw (1999).
6. S. W. Wu, C. J. Huang, B. G. Chen, and J. R. Ye, Ultrasonic detection primary, SNTCT (1988).
7. J. C. Liou, Ultrasonic testing of guided wave, NDT, 21, 9 (1999).
8. M. X. Xie, The Inspection of Defect in Pipelines Using Guided Waves, NSYSU (2003).
9. X. Jian, S. Dixon, and R. S. Edwards, Modelling ultrasonic generation for Lorentz force EMATs, Insight 46, 671–673 (2004).
10. X. Jian, S. Dixon, and S. B. Palmer, In–plane and out–of–plane particle velocity measurement using electromagnetic acoustical transducers, Proceeding of the IEEE Ultrasonic Symposium, pp.1276-1279 (2005).
11. Y. S. Zhang, Detection system about steel cracks based on electronic ultrasonic, NDT, 31, 4 (2009).
12. X. Jian , S. Dixon, K. Quirka, K.T.V. Grattan, Electromagnetic acoustic transducers for in- and out-of plane ultrasonic wave detection, Sensors and Actuators A 148 51 – 56 (2008).